A recombinant adenovirus type 35 fiber knob protein sensitizes lymphoma cells to rituximab therapy

Hongjie Wang,[1] Ying Liu,[1] Zong-Yi Li,[1] Xiaolong Fan,[2] Akseli Hemminki,[3] and André Lieber[1,4]

[1]Division of Medical Genetics, University of Washington, Seattle; [2]The Rausing Lab and Lund Strategic Research Center for Stem Cell Biology and Cell Therapy, Lund, Sweden; [3]Cancer Gene Therapy Group, University of Helsinki, Helsinki, Finland; and [4]Department of Pathology, University of Washington, Seattle

Many tumors, including lymphomas, upregulate expression of CD46 to escape destruction by complement. Tumor cells are therefore relatively resistant to therapy by monoclonal antibodies, which act through complement-dependent cytotoxicity (CDC). From an *Escherichia coli* expression library of adenovirus type 35 fiber knob mutants, we selected a variant (Ad35K^{++}) that had a higher affinity to CD46 than did the natural Ad35 fiber knob. We demonstrated that incubation of lymphoma cells with recombinant Ad35K^{++} protein resulted in transient removal of CD46 from the cell surface. Preincubation of lymphoma cells with Ad35K^{++} sensitized cells to CDC, triggered by the CD20-specific monoclonal antibody rituximab. In xenograft models with human lymphoma cells, preinjection of Ad35K^{++} dramatically increased the therapeutic effect of rituximab. Blood cell counts and organ histology were normal after intravenous injection of Ad35K^{++} into mice that express human CD46. The presence of polyclonal anti-Ad35K^{++} antibodies did not affect the ability of Ad35K^{++} to enhance rituximab-mediated CDC in in vitro assays. The Ad35K^{++}-based approach has potential implications in monoclonal antibody therapy of malignancies beyond the combination with rituximab. (Blood. 2010;115:592-600)

Introduction

Monoclonal antibodies (mAbs) have emerged as a class of novel oncology therapeutics. To date, there are 27 marketed therapeutic mAbs, including 10 specific for malignant disease, and there are hundreds of mAbs currently in clinical development. Among the mAbs approved by the Food and Drug Administration (FDA) for hematologic malignancies is rituximab (Mabthera, Rituxan). Rituximab is a humanized unconjugated immunoglobulin G1 mAb against CD20. CD20 is expressed on the surface of normal B lymphocytes and B-cell lymphoma but not on hematopoietic stem cells, pro-B cells, and plasma cells. Rituximab is currently used for the treatment of B-cell non-Hodgkin lymphoma (NHL), mantle cell lymphoma, hairy cell leukemia, chronic lymphocytic leukemia. The most common B-cell lymphoid cancer is NHL, with an estimated 66 120 new cases of B-cell NHL diagnosed in 2008, and an estimated 19 160 deaths from this disease occurred last year in the United States (http://www.cancer.org/downloads/STT/2008CAFFfinalsecured.pdf). Notably, since the introduction of rituximab therapy for B-cell NHL, the 5-year survival rate increased only 16%, from 48% (1975-1977) to 64% (1996-2003), indicating that many patients are or become resistant to rituximab treatment.

Therapeutic mAbs often confer killing of tumor cells by several mechanisms, including blocking and/or deregulating vital survival pathways and stimulating immune effector mechanisms, that is, antibody-dependent cell-mediated cytotoxicity and complement-dependent toxicity (CDC). A series of studies have shown that rituximab is effective in inducing CDC on B-cell lymphoma cells.[1-6] The therapeutic potential of rituximab is significantly limited because of the ability of hematopoietic malignancies to block CDC by the overexpression of membrane complement regulatory proteins, such as CD46, CD55, and CD59.[7-9] Several preclinical studies have shown that tumor cells can be sensitized to rituximab-induced CDC by CD55 and/or CD59 blocking antibodies.[10,11] A similar effect was seen with antisense oligonucleotides against CD55 and CD46, whereby these studies showed a predominant role of CD46 in protection of tumor cells against CDC.[12] In addition to blocking complement activation, CD55 and CD59 are also involved in T-cell activation.[13,14] This might give tumor cells that lost these 2 proteins a selective advantage in escaping immune-mediated destruction and might explain why CD55 and CD59 are often absent on tumors.[8] Therefore, it is generally thought that CD46 alone can protect tumor cells from complement lysis.[15] Because of this, as well as the observation that CD46 is uniformly expressed at high levels on many malignancies,[8,16-21] including hematologic malignancies,[8,9] our strategy to sensitize tumor cells to mAbs is centered on CD46.

CD46, a membrane-linked glycoprotein that is expressed on all cells except red blood cells, attaches to complement fragments C3b and C4b that are bound to host cells and then serves as a cofactor for their targeted destruction by the plasma serine protease factor I (reviewed in Liszewski et al[22]). CD46 is also a receptor for several pathogens, including measles virus, *Neisseria gonorrhoeae* and *Neisseria meningitides*, group A *Streptococcus*, and human herpes virus 6. We and others reported that CD46 is a high-affinity receptor for a series of human adenovirus (Ad) serotypes.[23-25] Among the serotypes that use CD46 is serotype 35. Ad35 engages CD46 by residues in the C-terminal trimeric fiber knob domain.[24] More recently, using an expression library of Ad35 fiber knob with

Submitted May 15, 2009; accepted October 19, 2009. Prepublished online as *Blood* First Edition paper, November 12, 2009; DOI 10.1182/blood-2009-05-222463.

The online version of this article contains a data supplement.

The publication costs of this article were defrayed in part by page charge payment. Therefore, and solely to indicate this fact, this article is hereby marked "advertisement" in accordance with 18 USC section 1734.

random mutations, we found that the amino acid residues within the Ad35 knob that mediate binding to CD46 are localized on 2 opposite ends of the fiber knob.[26] This implies that 1 CD46 monomer binds between 2 Ad35 knob monomers. This, together with the trimeric structure of the Ad35 knob, leads to a tight association with CD46 and cross-linking of several CD46 molecules. Using the Ad35 fiber knob *Escherichia coli* expression library, we also identified a set of Ad35 knob mutants with increased affinity to CD46.[27] Although the K_D (equilibrium dissociation constant) of wild-type knob (Ad35K) was 14.64nM, one of the selected mutants, Ad35K^{++}, containing a double Asp207Gly-Thr245Ala substitution, had a 23.2-fold higher affinity to CD46 (0.63 nM) (Figure 1A). The recombinant Ad35K^{++} protein can efficiently be produced in soluble form in *E coli* and purified by affinity chromatography. In this study, we show that incubation of tumor cells with Ad35K^{++} leads to transient CD46 internalization, which in turn sensitizes cells to rituximab-mediated CDC in vitro and in animal models for lymphoma.

Methods

Production of fiber knobs

Ad35 fiber knobs with increased affinity to CD46 were selected from an *E coli* expression library.[27] The knob domains were produced in *E coli* with N-terminal tags of 6 consecutive histidine residues and purified by Ni-NTA agarose chromatography as described elsewhere.[26] The fiber knob proteins were dialyzed against 20mM HEPES, 200mM NaCl, 17% glycerol. Endotoxin tests were performed with the Limulus Amebocyte Lysate test kit from Cape Cod Inc. For in vivo studies, preparations of recombinant Ad35K^{++} with less than 0.25 EU/mL endotoxin were used.

Cells

Human lymphoma cell lines Raji (ATCC CCL-86), Mino (ATCC CRL-300), Farage (ATCC CRL-2630), and BJAB cells (obtained from Edward A. Clark, University of Washington) were cultured in RPMI supplemented with 10% FBS and with L-glutamine and penicillin/streptomycin. Culture conditions for primary chronic lymphocytic leukemia cells are described in the supplemental information (available on the *Blood* website; see the Supplemental Materials link at the top of the online article). Peripheral blood mononuclear cells (PBMCs) from healthy donors were provided by Nora Disis (Tumor Vaccine Group, Department of Oncology, University of Washington).

Antibodies

Rituximab was from Genentech Inc. Daclizumab was from Roche Pharmaceuticals. All antibodies and conditions used for immunofluorescence and flow cytometric studies are described in the supplemental text.

Image acquisition

After washing, the slides were mounted with Vectashield containing DAPI (Vector Laboratories). Immunofluorescence microphotographs were taken on a Leica DMLB microscope (40× oil lens; Leica) with a Leica DFC300FX digital camera and Leica Application Suite Version 2.4.1 R1 (Figures 1D-I, 3A, 4A, and supplemental Figure 3; Leica Microsystems). Confocal microphotographs were taken on a Zeiss LSM 510 microscope and processed with Zeiss 510 software (supplemental Figure 2; Zeiss MicroImaging).

Ad35 infection studies

The Ad35-GFP vector has been described previously.[28] For transduction studies, 2×10^5 cells were incubated with PBS or 20 μg/mL Ad35K or Ad35K^{++} knob in 200 μL of medium at room temperature for 1 hour. Then cells were washed twice with PBS and incubated with fresh media at 37°C.

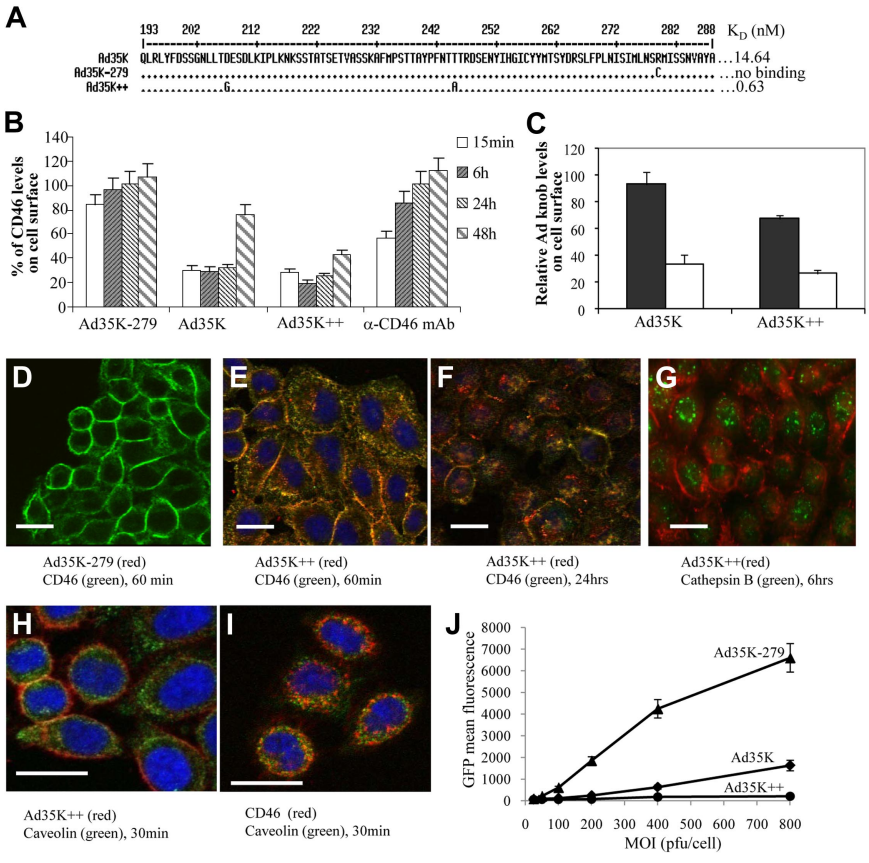

Figure 1. Ad35 knob interaction with CD46. (A) Partial amino acid sequence of wild-type fiber knob (Ad35K) and the Ad35 knob mutants Ad35K-279 (ablated for CD46 binding) and Ad35K^{++}. The corresponding affinities are indicated. The localization of the critical amino acid residues within a 3-dimensional model of the Ad35 fiber knob domain has been reported recently.[26,27] (B) CD46 surface levels. Raji cells were incubated with 20 μg/mL Ad35K-279, Ad35K, Ad35^{++}, or with anti-CD46 mAb. At the indicated time points, surface CD46 levels of cells were analyzed by flow cytometry. Shown is the percentage of CD46 levels (mean values and standard deviations), compared with CD46 mean fluorescence intensity of PBS-treated cells; n > 6; $P = .021$ for Ad35K versus Ad35K^{++} samples (15 minutes, 6 hours, 24 hours, and 48 hours combined). (C) Ad35 knob surface levels. Raji cells were incubated with Ad35K or Ad35K^{++} at room temperature for 1 hour. After washing with PBS, cells were incubated with fresh medium at 37°C for 15 minutes (■) or 6 hours (□). The levels of cell-bound Ad35 knob were analyzed by flow cytometry with the use of a mouse anti-His tag antibody followed by an anti–mouse antibody conjugated with Alexa Fluor 488. Shown is the fluorescence intensity (mean values and SDs); n > 6. (D-I) Immunofluorescence microscopy analysis of CD46, Cy3-Ad35K^{++}, cathepsin B, and caveolin. For better clarity of cytoplasmic signals, the microphotographs shown are from HeLa cells. Similar results were obtained with Raji cells. (J) Inhibition of Ad35-GFP infection. Raji cells were treated with 20 μg/mL Ad35K-279, Ad35K, or Ad35K^{++} for 24 hours and, after washing, infected with Ad35-GFP at the indicated MOIs (multiplicities of infection). GFP expression was analyzed 24 hours later. Shown are the mean values and SDs; n = 3.

After 2 hours of incubation, cells were infected with Ad35-GFP. Virus containing medium were substituted 2 hours after infection. Twenty-four hours after infection, GFP expression was analyzed by flow cytometry.

In vitro viability assays

Raji cells (5×10^4/well) were plated in triplicate in 96-well plates with RPMI complemented with 10% heat-inactivated FBS, preincubated with PBS, 25 μg/mL CD46 antibody (MEM-258; Serotec), or 25 μg/mL Ad35 knob proteins. Eight hours later, 15 μg/mL rituximab was added to cells and incubated at room temperature for 30 minutes. Normal human serum (NHS) was added to a final dilution of 1:5, and cells were incubated at 37°C for another 3 hours. Viable cells in each well were counted after trypan blue staining. Each sample was in triplicate, and each well was counted 4 times. Three independent studies were performed. The assay conditions for other cell types are described in the supplemental information.

Animal studies

All experiments involving animals were conducted in accordance with the institutional guidelines set forth by the University of Washington and were approved by the University Institutional Animal Care and Use Committee. Mice were housed in specific-pathogen–free facilities. To establish the xenograft lymphoma model, 3.5×10^6 Raji cells or 5×10^6 Farage cells in 200 μL of PBS was injected into the tail vein of immunodeficient severe combine immunodeficient (SCID)/beige (C.B-17/IcrHsd-scid-bg) mice. For survival studies, animals were checked every 12 hours. The end point for Kaplan-Meier studies was the onset of hind leg paralysis or morbidity. For immunization studies with Ad35 fiber knobs, CD46 transgenic C57Bl/6 mice line MCP8B received 3 subcutaneous injections of 5 μg Ad35K^{++} knob at days 0, 3, and 6. Serum was collected 4 weeks later and analyzed for Ad-specific antibodies by Western blot.

Results

Removal of CD46 from cell surface

Flow cytometric studies showed high and relatively uniform levels of CD46 on primary chronic lymphocytic leukemia (B-CLL) cells and test lymphoma cell lines (supplemental Figure 1). We first studied the effect of Ad35K^{++} on CD46 levels in Raji cells, a CD20$^+$, human Burkitt lymphoma cell line.

Flow cytometry showed that incubation of Raji cells with Ad35K^{++} resulted in a 90% decrease of CD46 levels within 6 hours, after which surface CD46 was restored (Figure 1B). The effect of the wild-type Ad35 fiber knob (Ad35K) was significantly less pronounced. No decrease in CD46 levels was seen with an Ad35 knob that was ablated for CD46 binding (Ad35K-279) or with a mAb specific to a CD46 epitope different from that of the anti-CD46 detection antibody. Together with a decrease of surface CD46, we also found less cell-bound Ad35K and Ad35K^{++} knob after 6 hours of incubation, indicating that CD46 and Ad35 knobs are taken up together (Figure 1C).

Immunofluorescence microscopy for CD46 and Ad35K^{++} knob further corroborated less surface CD46 in Ad35K^{++}-treated cells compared with cells incubated with Ad35K-279 at 30 minutes (supplemental Figure 2) and 60 minutes (Figure 1D-E) after adding knob proteins. At 12 hours (supplemental Figure 2) or 24 hours (Figure 1F), cells treated with Ad35K^{++} showed predominantly cytoplasmic CD46 staining, whereby it appeared that CD46 signals were less than before incubation, indicating degradation of internalized CD46-Ad35K^{++}. CD46 reappeared on the cell surface by 48 hours (supplemental Figure 2). Internalized CD46 and Ad35K^{++} did not colocalize with the late endosomal marker cathepsin B (Figure 1G; supplemental Figure 3A). Instead both proteins costained with caveolin, an early endosomal marker at early time points (Figure 1H-I; supplemental Figure 3B). Taken together, this indicates that the internalized CD46-Ad35K^{++} complex is either directly released from early endosomes to the cytosol or sorted to a compartment different from late endosomes or lysosomes, where subsequent degradation occurs. Overtime, de novo produced CD46 reappears on the cell surface.

Previous studies have shown that transduction with Ad35 fiber–containing Ad vectors directly correlates with the density of CD46 on the cell surface.[29] In transduction studies with a GFP-expressing Ad35 vector (Ad35-GFP) that uses CD46 for infection, we found that preincubation of Raji cells with Ad35K^{++} decreased GFP expression levels more than 1000-fold, compared with cells incubated with Ad35K-279 (Figure 1J). Note that the nonmutated Ad35K protein conferred less protection from Ad35-GFP infection.

Taken together, these studies show that Ad35K^{++} incubation of Raji cells results in transient removal of CD46 from the cell surface.

Incubation of lymphoma cells with Ad35K^{++} sensitizes them to rituximab-mediated CDC in vitro

We then studied whether Ad35K^{++} incubation would render lymphoma cells more susceptible to CDC induced by rituximab. Initial experiments were done with Raji cells (Figure 2A). Incubation of Raji cells with rituximab followed by NHS, used as a source of complement, resulted in killing of approximately 70% of Raji cells within 3 hours (Figure 2A, PBS/rituximab + NHS). Note that the remaining viable Raji cells had CD20 levels that were approximately 50-fold lower than the mean CD20 fluorescence level of the control population (no rituximab or no NHS). To test whether the efficacy of rituximab-mediated CDC can be increased by Ad35K^{++}-triggered internalization of CD46, we incubated Raji cells with Ad35K-279, Ad35K, and Ad35K^{++} for 8 hours. Ad35K and Ad35K^{++} increased rituximab/NHS-mediated cell killing by approximately 2- and 10-fold, respectively, compared with rituximab/NHS alone. The sensitizing effect of Ad35K^{++} was seen at doses as low as 25 ng/mL (supplemental Figure 4). Ad35K-279 had no effect on rituximab/NHS-mediated killing. Preincubation of Raji cells with anti-CD46 mAb in combination with rituximab/NHS was significantly less efficient than preincubation with Ad35K or Ad35K^{++} (anti-CD46 mAb versus Ad35K, $P = .024$). In addition, the enhancing effect on rituximab CDC in vitro is significantly greater for Ad35K^{++} than for Ad35K ($P < .02$). Incubation of Raji cells with Ad35K or Ad35K^{++} together with NHS caused an approximately 30% decline in cell viability, most likely as a result of CDC when CD46 is blocked. To test the specificity of rituximab-mediated CDC of CD20$^+$ lymphoma cells, we used the humanized mAb daclizumab that binds to CD25, which is not expressed on Raji cells (data not shown). There was no significant cell killing mediated by this antibody when combined with NHS (Figure 2A).

To consolidate our findings on Raji cells, we performed studies with other CD20$^+$ lymphoma cell lines, including BJAB (Epstein-Barr virus–negative Burkitt lymphoma), Farage (non-Hodgkin B-cell lymphoma), and Mino (mantle cell lymphoma). In all cell lines tested we found a significant increase in rituximab/NHS-mediated cell killing when cells were preincubated with Ad35K^{++} (Figure 2B). Furthermore, we used primary cells from patients with B-CLL (Figure 2C). Preincubation of B-CLL cells with Ad35K^{++} knob significantly increased the efficacy of rituximab/NHS treatment. Notably, the cell sample that was most resistant to Ad35K^{++}/rituximab killing (CCL-3) had the lowest percentage of CD20$^+$ cells and the lowest CD20 levels (see supplemental Figure 1).

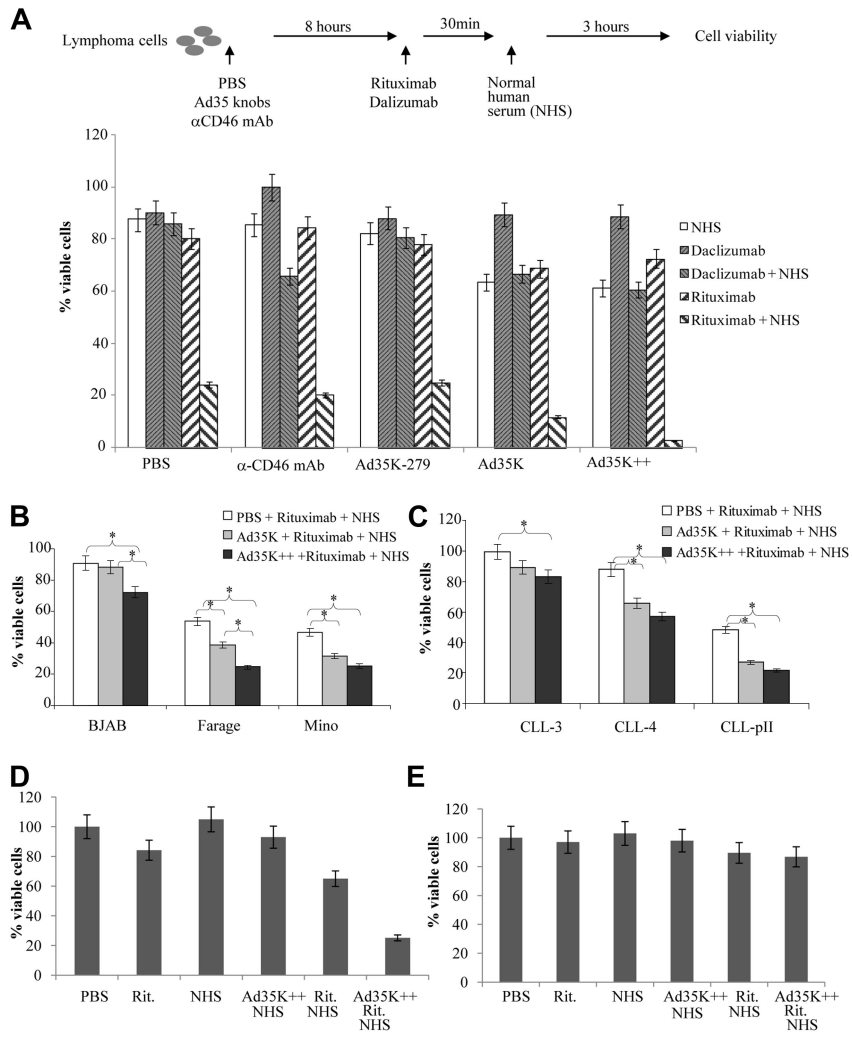

Figure 2. Ad35K^{++}-sensitized cytolysis of lymphoma cells in vitro. (A top) Scheme of the experiment with Raji cells. Raji cells were incubated with anti-CD46 mAb, Ad35K-279, Ad35K, or Ad35K^{++}. Eight hours later, daclizumab or rituximab were added to cells and incubated at room temperature. After 30 minutes, NHS was added, and viable cells were counted 3 hours later based on trypan blue exclusion. (Bottom) Percentage of viable cells compared with PBS-treated cells. Shown are the mean values and standard deviations; n > 6. (B-C) Studies with other lymphoma cell lines (B) or primary cells from patients with B-CLL (C). The experimental conditions were as described in panel A. Significant differences ($P < .05$) are marked by an asterisk. (D) Studies with normal human PBMCs. Human PBMCs (pooled from 3 healthy donors) were sorted for CD20$^+$ cells with the use of fluorescence-activated cell sorting. CD20$^+$ cells were cultured for 3 days. A total of 10^5 cells were treated with Ad35K^{++} (25 μg/mL), followed by rituximab (15 μg/mL) and NHS (25% final concentration) 8 hours later. Four hours after adding NHS, viable cells were counted based on trypan blue exclusion. Cell viability of PBS-treated cells was taken as 100%. There was no change in cell viability for cells incubated with Ad35K^{++}, rituximab, or NHS alone. (E) Human PBMCs were cultured for 3 days and treated as described in panel D. Shown are the mean values and standard deviations; n = 5.

As outlined in the Introduction, CD20 is expressed on mature human B cells. We therefore tested the cytotoxicity of our approach on normal human B cells. When incubated with CD20$^+$ cells sorted from normal human PBMCs, we found that rituximab killed 15% of the cells and that the addition of NHS increased the percentage of dead CD20$^+$ cells to 35%, compared with PBS-treated cells ($P < .05$; Figure 2D). Preincubation with Ad35K^{++} resulted in rituximab/NHS-mediated killing of approximately 75% of primary CD20$^+$ cells. Ad35K^{++} incubation alone did not kill CD20$^+$ PBMCs. The combination of Ad35K^{++} and NHS resulted in a nonsignificant decline in cell viability ($P = .12$).

When total PBMCs were tested, no significant decrease in cell viability was observed after incubation with rituximab/NHS and Ad35K^{++}/rituximab/NHS (Figure 2E), although incubation with Ad35K^{++} caused a decrease in surface CD46 levels on PBMCs (supplemental Figure 5). To further analyze the specificity of Ad35K^{++}/rituximab/NHS killing, we performed in vitro studies with a series of primary human cell cultures, including vascular endothelial cells, cornea epithelial cells, ovarian surface epithelial cells, and foreskin fibroblasts (supplemental Figure 6). Incubation of cells with rituximab/NHS did not cause cell death, which is not surprising because these cell types do not express CD20. Notably, Ad35K^{++}/NHS and Ad35K^{++}/rituximab/NHS resulted in an insignificant decline of cell viability. Similar data were obtained after incubation of CD20$^-$-transformed cell lines such as HeLa (cervical cancer), Mo7e (erythroleukemia), BT474 (breast cancer), SK-BR3 (breast cancer), A549 (lung cancer), and HT-29 (colon cancer) cells with rituximab, Ad35K^{++}/NHS, or Ad35K^{++}/rituximab/NHS (data not shown).

In summary, the in vitro studies show that Ad35K^{++} preincubation of primary CD20$^+$ PBMCs, primary B-CLL cells, and lymphoma cell lines increases the cytotoxicity of rituximab. No significant Ad35K^{++}-mediated complement-mediated killing of primary CD20$^-$ cells was observed.

Ad35K^{++} improves antitumor efficacy of rituximab in vivo

To establish a xenograft lymphoma model, we intravenously injected Raji cells into immunodeficient CB17-SCID/beige mice. At different time points after injection, mice were killed, and peripheral white blood cells, splenocytes, cells from mesenteric lymph nodes, and bone marrow cells were analyzed for the presence of Raji cells by flow cytometry for human CD20 and immunofluorescence microscopy. HuCD20$^+$ Raji cells were predominantly found in the bone marrow and lymph nodes and were sparse in the spleen (Figure 3A). The percentage of huCD20$^+$ cells increased from 20% plus or minus 4% (bone marrow) and 5% plus or minus 1.2% (lymph nodes) at day 10 after Raji cell injection to 75% plus or minus 6% and 42% plus or minus 8% at day 14 after injection. At days 15 or 16 after Raji cell injection, mice developed hind leg paralysis, a symptom that we eventually used as an end point in Kaplan-Meier

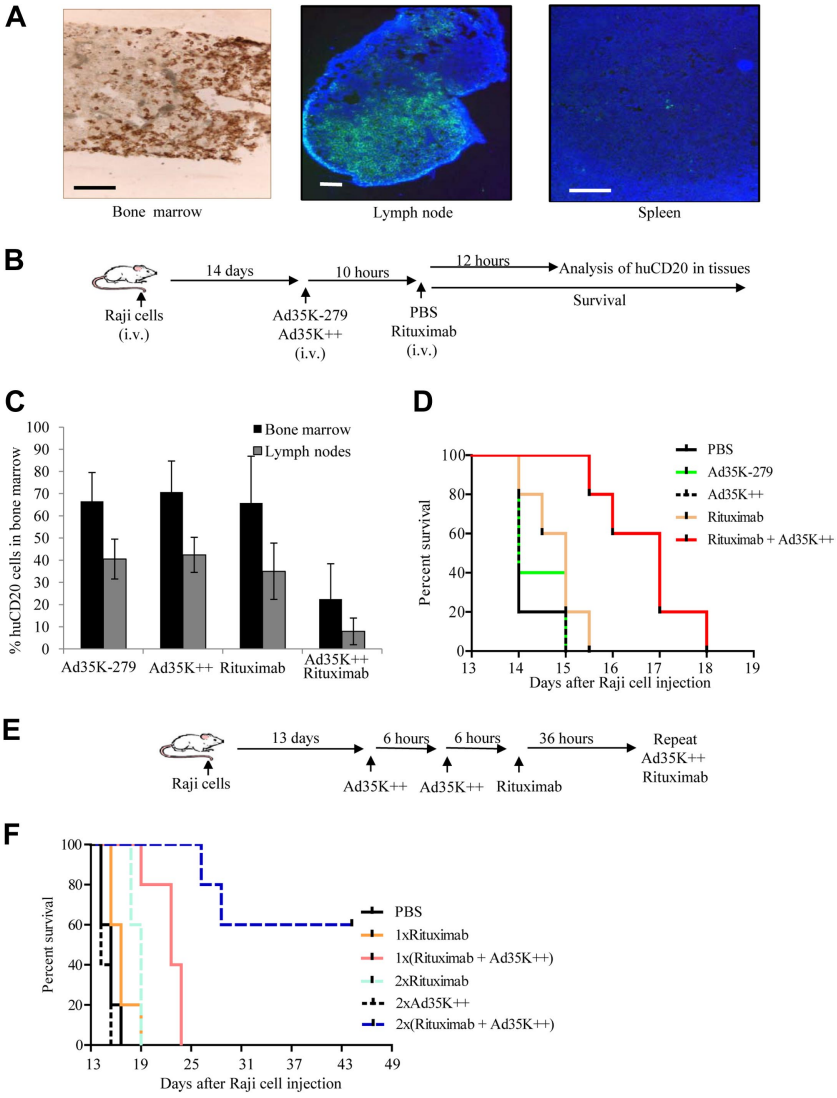

Figure 3. Effect of Ad35K^{++} in Raji lymphoma xenograft model. (A) Distribution of human CD20^{+} Raji cells. At day 14 after intravenous Raji cell injection, femurs, spleens, and mesenteric lymph nodes were harvested. Lymph node and spleen sections were analyzed by immunofluorescence microscopy with FITC-labeled anti–human CD20 antibodies. For bone sections, the Klear Mouse DAB detection kit (Golden Bridge International Inc) was used. Positive staining appears in brown. Specificity of staining was confirmed by staining with corresponding isotype-matched antibodies (negative control) and antibodies specific to a human mitochondrial marker (positive control). Representative sections are shown. The scale bars represent 40 μm. (B) Scheme of experimental setting no. 1. CB17-SCID/beige mice received 3×10^6 human lymphoma Raji cells by tail vein injection. Fourteen days later, when control mice developed the first clinical symptoms, animals were intravenously injected with Ad35K-279 or Ad35K^{++}. Rituximab or PBS was given intravenously 10 hours later. In the first experiment, mice were killed 12 hours later, and tissues were analyzed for human CD20^{+} cells. In a second experiment, animals were monitored every 12 hours for onset of paralysis or morbidity, which served as the end point for Kaplan-Meier survival studies. (C) Percentage of human CD20^{+} Raji cells in bone marrow and mesenteric lymph nodes of treated mice measured by flow cytometry (12 hours after treatment); n = 5. The differences between rituximab and Ad35K^{++}/rituximab are significant ($P < .02$) for both, bone marrow and spleen. The differences between Ad35K-279, Ad35K^{++}, and rituximab are not significant. (D) Kaplan-Meier survival study; n = 10. (E) Scheme of experimental setting no. 2. At day 13 after lymphoma cell injection, the first treatment cycle was started with 2 intravenous injections of 50 μg of Ad35K^{++} 6 hours apart. Six hours after the second Ad35K^{++} injection, mice received an intravenous injection of 50 μg of rituximab. A second treatment cycle was started 36 hours later. Onset of hind leg paralysis served as an end point in survival studies. (F) Kaplan-Meier survival study. Mice received either 1 treatment cycle [1 × (rituximab + Ad35K^{++})] or 2 cycles [2 × (rituximab + Ad35K^{++})], or the indicated control injections; n = 10.

survival studies. For therapy studies, 14 days after implantation of Raji cells, mice received either 50 μg of (2.5 mg/kg) Ad35K^{++} or 50 μg of CD46-binding ablated Ad35K-279 protein (Figure 3B). Ten hours later, either PBS or 50 μg of rituximab was injected into the tail vein. One group of mice was killed 12 hours later, and the effect of Ad35K-279, Ad35K^{++}, rituximab, and Ad35K^{++}/rituximab on killing of Raji cells in vivo was measured, based on the percentage of huCD20^{+} cells in the bone marrow and lymph nodes (Figure 3C). Compared with Ad35K-279–treated control mice, no significant decrease in huCD20^{+} cell numbers was observed when Ad35K^{++} or rituximab was injected alone. However, the combination of Ad35K^{++} and rituximab resulted in a significant decrease in huCD20^{+} cells ($P < .03$). These findings were confirmed in survival studies (Figure 3D); there was a remarkable increase in survival when mice were treated with Ad35K^{++}/rituximab compared with rituximab only or Ad35K-279 treatment (rituximab versus Ad35K^{++}/rituximab, $P = .005$; Ad35K-279 versus Ad35K^{++}/rituximab, $P < .001$). There was no difference in survival between the control (PBS or Ad35K-279) and Ad35K^{++} only groups. Compared with the wild-type Ad35K protein, Ad35K^{++} exerted a significantly stronger enhancing effect on rituximab therapy (supplemental Figure 7). Rituximab at a dose of 2.5 mg/kg alone did not exert a significant therapeutic effect in vivo (Ad35K-279 versus rituximab, $P = .129$); however, a further increase to a dose of 12.5 mg/kg resulted in therapeutic efficacy (supplemental Figure 8). (Notably, doses from 2 to 25 mg/kg rituximab are used in clinical settings.) Furthermore, we tested several additional therapy schemes and found that an approach that involves 2 cycles of double Ad35K^{++} injection followed by rituximab application (Figure 3E) enabled long-term survival of mice that received a transplant with Raji lymphoma cells. Note that treatment was started at as advanced stage, that is, 3 days, before the control mice would die. Sixty percent of Raji lymphoma-bearing mice survived longer than 44 days (the time of follow-up) with treatment regiments of 2 times (rituximab + Ad35K^{++}), whereas all PBS-treated mice died within 16 days after Raji cell transplantation (Figure 3F).

Next, we tested our approach in a second tumor model that used the human NHL cell line Farage (Figure 4). Intravenous injection of 5×10^6 cells into CB17-SCID/beige mice resulted in onset of morbidity/paralysis at day 23. At this time, Farage cells had massively infiltrated the bone marrow, mesenteric lymph nodes, and spleen as shown by immunofluorescence microscopy with anti-huCD20 antibodies (Figure 4A). In these organs huCD20^{+} cells displayed a predominantly nodular neoplastic growth pattern, which is characteristic for follicular NHL in humans. Treatment of mice was started at day 21 after injection of Farage cells (Figure

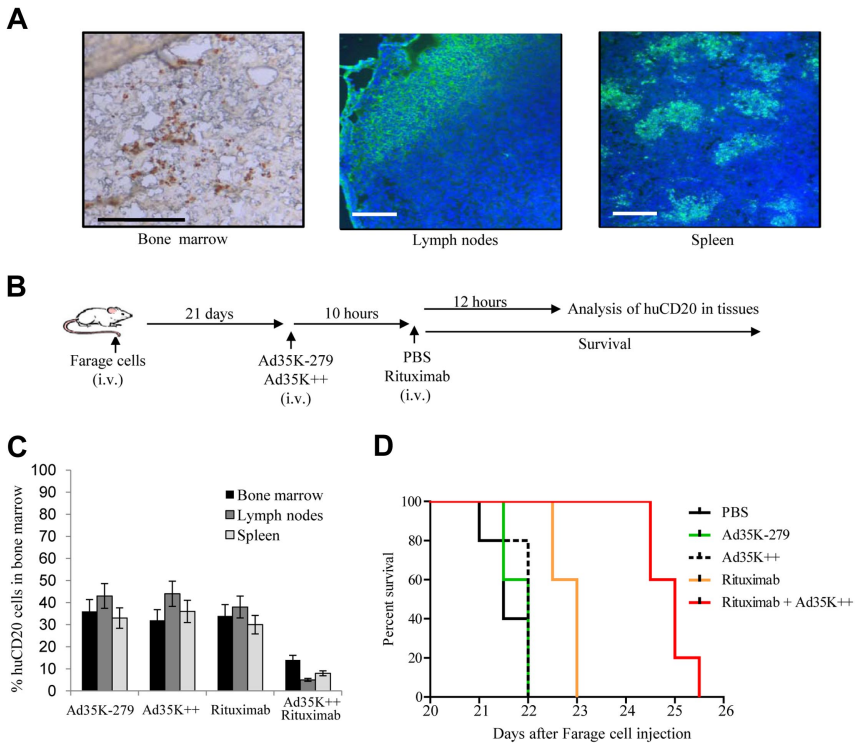

Figure 4. Effect of Ad35K^{++} on rituximab therapy in Farage xenograft model. (A) Distribution of human CD20^{+} Farage cells. Note the follicular tumor growth, particularly in the spleen. (B) Treatment scheme. Treatment was started at day 21 after intravenous injection of Farage cells. (C) Flow cytometry for huCD20 cells; n = 7. The differences between rituximab and Ad35K^{++}/rituximab are significant for all 3 tissues ($P < .03$). (D) Kaplan-Meier survival study after 1 round of treatment; n = 7.

4B). As seen with Raji cells, Ad35K^{++}/rituximab treatment resulted in a significant reduction of huCD20^{+} cells in all affected tissues compared with rituximab treatment alone ($P < .05$ for Ad35K^{++}/rituximab versus all other groups; Figure 4C-D). The median survival times for PBS-, rituximab-, and Ad35K^{++}/rituximab-treated mice were 25, 27, and 32 days, respectively. The difference between PBS and rituximab (P = .046) and rituximab and Ad35K^{++}/rituximab ($P < .02$) were significant. The differences between the remaining groups were not significant.

Safety and immunogenicity of intravenous Ad35K^{++} injection

Because in mice the homologue of CD46 is expressed only in the testis, transgenic mice that express huCD46 in a pattern and at levels similar to humans are a better model for safety studies. These CD46 transgenic mice have been used in toxicology studies for oncolytic measles virus, whereby the outcome of these studies was in concordance with the findings in monkeys[30] and humans (Evanthia Galanis [Mayo Clinic, Rochester, MN], oral communication, American Society for Stem Cell and Gene Therapy, May 2009) indicating that CD46 transgenic mice are an adequate model for testing CD46 ligands.

We intravenously injected the same dose of Ad35K^{++} that was used in the therapy studies into huCD46 transgenic, immunocompetent C57Bl/6 mice (strain MCP-8B).[31] Analyses of blood cell counts and other hematologic parameters at 16 and 48 hours after Ad35K^{++} injection did not show abnormalities (supplemental Table 1). At necropsy (day 14 after infection), no pathologic or histologic changes were found in all organs analyzed (brain, lung, heart, liver, kidney, intestines, bone marrow).

To assess the potential immunogenicity of Ad35K^{++} and the possibility for repeated injection in settings without immunosuppression, we measured Ad35K^{++}-specific antibodies in serum of patients with cancer. None of the 20 serum samples tested contained antibodies that reacted with either Ad35K or Ad35K^{++}. However, 18 serum samples contained antibodies specific to Ad5 hexon, Ad5 fiber knob, and Ad5 penton (Figure 5A). This outcome is not surprising. Although most humans have neutralizing antibodies against Ad5 virus, less than 10% of humans have neutralizing antibodies against Ad35 virus,[32] implying that Ad35K^{++} can be applied at least once in most humans. However, it is expected that injection of Ad35K^{++} will trigger the production of Ad35K^{++} antibodies in immunocompetent patients. In an attempt to assess whether anti-Ad35K^{++} antibodies affect Ad35K^{++}-mediated sensitization to rituximab therapy, we injected Ad35K^{++} into huCD46 transgenic mice. We compared a standard vaccination scheme involving 3 subsequent subcutaneous Ad35K^{++} injections with intravenous injection of Ad35K^{++} used in our in vivo studies before. Although we detected antibodies that reacted with Ad35K^{++} and, to a lesser degree, with Ad35K in mice that received Ad35K^{++} subcutaneously, no detectable antibodies were observed when Ad35K^{++} was given intravenously (Figure 5B). This is probably due to inefficient uptake of Ad35K^{++} by antigen-presenting cells after intravenous injection. We also used the serum from vaccinated or naive mice together with Ad35K^{++} in rituximab-mediated CDC assays. Regardless of the presence of anti-Ad35K^{++} antibodies, we found the same stimulating effect of Ad35K^{++} in cell killing (Figure 5C). This might be because the Ad35K^{++} interaction with CD46 is of high affinity and cannot be disrupted by polyclonal anti-Ad35K^{++} antibodies that develop in Ad35K^{++}-injected mice. The finding that Ad35K^{++}-induced antibodies reacted less with Ad35K than with Ad35K^{++} (see Figure 5B) was interesting, and we speculated that small conformational changes within the fiber knob can lead to loss or decrease of immunogenicity.

Overall, our data in huCD46 transgenic mice indicate that intravenous injection of Ad35K^{++} is safe and that repeated Ad35K^{++} application can potentially have a therapeutic effect in patients who do not receive immunosuppressive chemotherapy.

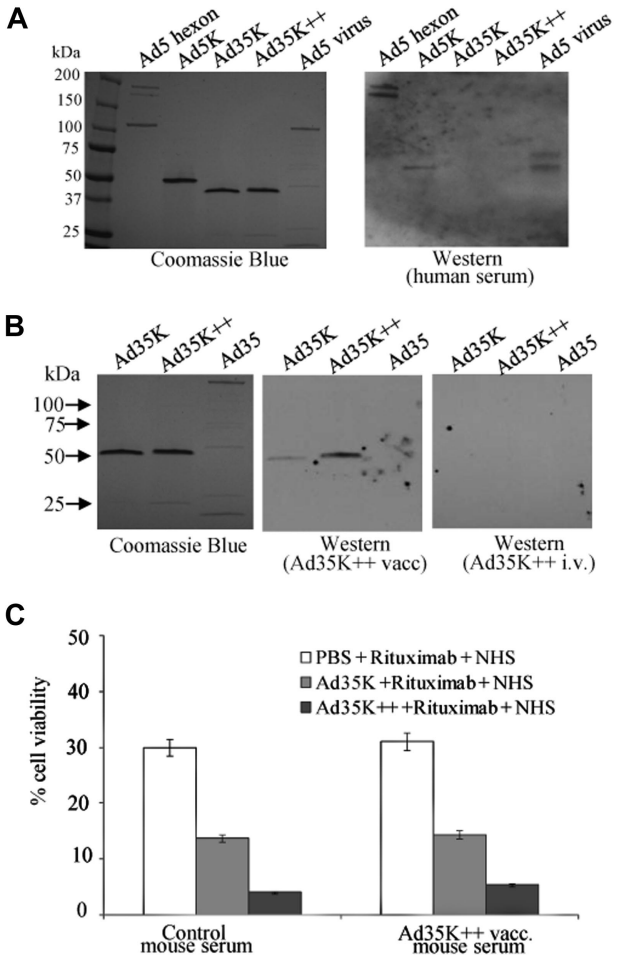

Figure 5. Immunogenicity of Ad35K^{++}. (A) Analysis of Ad knob-specific antibodies in serum from patients with cancer. Recombinant Ad5 hexon, Ad5 knob, Ad35K, and Ad35K^{++} as well as denaturated Ad5 particles were separated by polyacrylamide gel electrophoresis and stained with Coomassie blue (left). The proteins were plotted to nitrocellulose filter, which were incubated with human serum and subsequently with mouse anti–human immunoglobulin G–HRP conjugates (right). Human serum reacted with multimeric Ad5 hexon, trimeric Ad5 knobs, and virion pentons (~ 70- and 80-kDa bands) but not with Ad35K or Ad35K^{++}. Shown is a representative sample. (B) Analysis of knob antibodies in serum from mice that were injected subcutaneously with Ad35K^{++} (Ad35K^{++} vacc) or injected intravenously with Ad35K^{++} (Ad35K^{++} i.v.). Shown are representative samples. Photographs were taken with a digital Panasonic Lumix TZ-3 camera and processed in Adobe Photoshop. (C) Effect of anti-Ad35K^{++} serum on rituximab-mediated CDC. Raji cells were preincubated with mouse serum at a final dilution of 1:20 for 10 minutes at room temperature. Control serum was from normal mice. Test serum was from vaccinated mice that received subcutaneous Ad35K^{++} vaccinations. Then, 25 ng/mL Ad35K or Ad35K^{++} was added for 10 hours, followed by incubation with 15 μg/mL rituximab. CDC was induced 30 minutes later by adding NHS. Viable cells were counted 3 hours later. Shown are the mean values and SDs; n = 5.

Discussion

We generated a mutant Ad35 fiber knob (Ad35K^{++}) that binds to CD46 with high affinity (0.6nM) and cross-links several CD46 molecules on the membrane of cancer cells. Ad35K^{++} can be produced in soluble form in *E coli* and can be easily purified. Ad35K^{++} binding results in transient removal of CD46 from the surface of lymphoma cells for approximately 48 hours after treatment. During this time period, lymphoma cells that are normally resistant to rituximab become susceptible and can be killed by rituximab-mediated CDC in vitro. We then demonstrated in 2 murine lymphoma models that rituximab plus Ad35K^{++} achieved superior antitumor effects and animal survival compared with animals treated with rituximab alone.

Although a role of complement is clearly supported by data from in vitro and xenograft models,[1-6] the relevance of CDC in rituximab therapy in clinical settings is still controversial. Indirect proof of a role of CDC comes from clinical studies that show the consumption of human complement after rituximab administration.[33,34] In addition, preclinical studies showed that the antilymphoma effect of rituximab activity was completely abolished in C57Bl/6 mice lacking C1q, showing the role of complement activation in rituximab therapy in mice.[1] It is, however, undisputed that CDC plays a part in mediating the efficacy of rituximab through its ability to enhance antibody-dependent cell-mediated cytotoxicity, immune effector cell chemotaxis, and activation of antitumor T-cell responses.[33] A critical role of CDC in mAb therapy is also acknowledged by the fact that several biotechnology companies develop newer mAbs with increased ability to activate CDC,[35] such as ofatumumab, another CD20-specific mAb.[36] Furthermore, a role of CDC in tumor cell killing has been reported for alemtuzumab (an anti-CD52 mAb), which is used for treatment of chronic lymphocytic leukemia,[37] for gemtuzumab (an anti-CD33 mAb), used for treatment of acute myeloid leukemia,[38] as well as for panitumumab and cetuximab (anti-EGFR mAbs), used for the treatment of colon cancer.[39] Overall, this indicates that the Ad35K^{++}-based adjuvants approach has implications in mAb therapy beyond the combination with rituximab.

We demonstrated therapeutic efficacy of Ad35K^{++}/rituximab treatment in immunodeficient mice, indicating that T and B cells are not involved in tumor cell killing. This suggests that the Ad35K^{++}/rituximab approach will also be efficient in immunosuppressed patients, ie, patients who receive chemotherapy. Notably, the combination of rituximab with myeloreductive chemotherapy is often used clinically and has been shown to prolong progression-free survival in patients with NHL.[40] However, chemotherapy is also associated with leukopenia and proneness to infection; therefore, approaches to increase rituximab efficacy without the need of immunosuppression are desirable. Although our preliminary data suggest that polyclonal anti-Ad35K^{++} antibodies cannot interfere with the high-affinity interaction between Ad35K^{++} and CD46 on lymphoma cells, it remains to be tested whether repeated Ad35K^{++}/rituximab application is efficient in immunocompetent models. This, however, requires the generation of double transgenic huCD20/CD46 mice and syngeneic lymphoma cells. Ultimately, this model would also be required for dose-response studies in preparation of potential clinical trials.

Rituximab/NHS also killed primary CD20^{+}-PBMCs, which was enhanced by preincubation with Ad35K^{++}. This side effect has to be considered in clinical settings. However, the enhancing effect of Ad35K^{++} on rituximab killing of primary B cells has practical implications because rituximab is currently used in patients to treat autoimmune diseases[41,42] and acute antibody-mediated rejection of transplants.[43] Ad35K^{++} injection did not cause toxic side effects after intravenous injection into C57Bl/6 transgenic mice expressing human CD46 in a pattern and at a level similar to humans. Because the murine analog of human CD46 is only expressed in the testes of these mice and because it is unknown whether huCD46 prevents CDC in mice, the lack of toxicity by Ad35K^{++} in our studies does not necessarily predict its safety in humans. Studies on PBMCs and CD20^{-} primary human cells have shown, however, that incubation with Ad35K^{++}/NHS caused only minimal toxicity, although Ad35K^{++} treatment of PBMCs triggered the removal of CD46

from the cell surface. Notably, human PBMCs, in contrast to Raji cells, express high levels of 2 other membrane complement regulatory proteins, CD55 and CD59, which can protect them from CDC (data not shown). Furthermore, the density of CD46 on primary cells is at least one order of magnitude lower than on lymphoma cells (supplemental Figure 1). Subsequent to incubation with Ad35K^{++}, the mean CD46 fluorescence intensity decreased only 1.97 plus or minus 0.21-fold on PBMCs, whereas it declined by 7.54 plus or minus 0.35-fold on Raji cells. Note that we used an Ad35K^{++} concentration in our in vitro assay (5×10^8 Ad35K^{++} knob molecules per cell; see supplemental Figure 4) that is unlikely to be achieved after intravenous Ad35K^{++} injection in vivo.

Measles virus can cause immunosuppression either by direct binding of the virus to CD46 or by interaction of C3b/C4b-opsonized immune complexes with CD46. However, this mechanism cannot be generalized to all CD46-interacting ligands. The outcome of CD46 ligation depends on the CD46 isoform with which the ligand interacts as well as the domain within CD46 that is used for binding. In addition, to generate immunosuppressive T cells, the ligation of both the T-cell receptor and CD46 is required. Studies in transgenic mice and nonhuman primates showed that injection of anti-CD46 mAbs as well as CD46-targeting Ad5/35 or Ad35 virus vectors had no detrimental effects on the host's immune system,[31,44-46] suggesting that the Ad35K^{++}/rituximab approach will not cause immunosuppression.

In summary, this preclinical study shows efficacy and safety of a new approach to enhance rituximab-based therapy of lymphoma and, potentially, of autoimmune diseases and transplant rejection. Considering the central role of CDC in mAb cancer therapy, Ad35K^{++} might also be beneficial in combination with other mAbs specific to other types of cancer.

Acknowledgments

We thank Qinghua Feng and Nancy Kiviat for providing patient serum and Ruan van Rensburg for editing the manuscript. We also thank Nelly Auersperg and the Canadian Ovarian Tissue Bank for providing human ovarian surface epithelial cells.

The study was supported by National Institutes of Health grants HLA078836 and CA080193 and by the Life Science Discovery Fund.

Authorship

Contribution: H.W., Y.L., Z.-Y.L., and A.L. performed the experiments; X.F. and A.H. provided material; and A.L. wrote the paper.

Conflict-of-interest disclosure: The authors declare no competing financial interests.

Correspondence: André Lieber, University of Washington, Division of Medical Genetics, Box 357720, Seattle, WA 98195; e-mail: lieber00@u.washington.edu.

References

1. Di Gaetano N, Cittera E, Nota R, et al. Complement activation determines the therapeutic activity of rituximab in vivo. *J Immunol.* 2003;171(3):1581-1587.
2. Golay J, Cittera E, Di Gaetano N, et al. The role of complement in the therapeutic activity of rituximab in a murine B lymphoma model homing in lymph nodes. *Haematologica.* 2006;91(2):176-183.
3. Reff ME, Carner K, Chambers KS, et al. Depletion of B cells in vivo by a chimeric mouse human monoclonal antibody to CD20. *Blood.* 1994;83(2):435-445.
4. Bellosillo B, Villamor N, Lopez-Guillermo A, et al. Complement-mediated cell death induced by rituximab in B-cell lymphoproliferative disorders is mediated in vitro by a caspase-independent mechanism involving the generation of reactive oxygen species. *Blood.* 2001;98(9):2771-2777.
5. van der Kolk LE, Grillo-Lopez AJ, Baars JW, Hack CE, van Oers MH. Complement activation plays a key role in the side-effects of rituximab treatment. *Br J Haematol.* 2001;115(4):807-811.
6. Harjunpaa A, Junnikkala S, Meri S. Rituximab (anti-CD20) therapy of B-cell lymphomas: direct complement killing is superior to cellular effector mechanisms. *Scand J Immunol.* 2000;51(6):634-641.
7. Fishelson Z, Donin N, Zell S, Schultz S, Kirschfink M. Obstacles to cancer immunotherapy: expression of membrane complement regulatory proteins (mCRPs) in tumors. *Mol Immunol.* 2003;40(2-4):109-123.
8. Hara T, Kojima A, Fukuda H, et al. Levels of complement regulatory proteins, CD35 (CR1), CD46 (MCP) and CD55 (DAF) in human haematological malignancies. *Br J Haematol.* 1992;82(2):368-373.
9. Ong HT, Timm MM, Greipp PR, et al. Oncolytic measles virus targets high CD46 expression on multiple myeloma cells. *Exp Hematol.* 2006;34(6):713-720.
10. Ziller F, Macor P, Bulla R, Sblattero D, Marzari R, Tedesco F. Controlling complement resistance in cancer by using human monoclonal antibodies that neutralize complement-regulatory proteins CD55 and CD59. *Eur J Immunol.* 2005;35(7):2175-2183.
11. Guo B, Ma ZW, Li H, et al. Mapping of binding epitopes of a human decay-accelerating factor monoclonal antibody capable of enhancing rituximab-mediated complement-dependent cytotoxicity. *Clin Immunol.* 2008;128(2):155-163.
12. Zell S, Geis N, Rutz R, Schultz S, Giese T, Kirschfink M. Down-regulation of CD55 and CD46 expression by anti-sense phosphorothioate oligonucleotides (S-ODNs) sensitizes tumour cells to complement attack. *Clin Exp Immunol.* 2007;150(3):576-584.
13. Hamann J, Stortelers C, Kiss-Toth E, Vogel B, Eichler W, van Lier RA. Characterization of the CD55 (DAF)-binding site on the seven-span transmembrane receptor CD97. *Eur J Immunol.* 1998;28(5):1701-1707.
14. Deckert M, Kubar J, Bernard A. CD58 and CD59 molecules exhibit potentializing effects in T cell adhesion and activation. *J Immunol.* 1992;148(3):672-677.
15. Madjd Z, Durrant LG, Pinder SE, et al. Do poor-prognosis breast tumours express membrane cofactor proteins (CD46)? *Cancer Immunol Immunother.* 2005;54(2):149-156.
16. Rushmere NK, Knowlden JM, Gee JM, et al. Analysis of the level of mRNA expression of the membrane regulators of complement, CD59, CD55 and CD46, in breast cancer. *Int J Cancer.* 2004;108(6):930-936.
17. Varela JC, Atkinson C, Woolson R, Keane TE, Tomlinson S. Upregulated expression of complement inhibitory proteins on bladder cancer cells and anti-MUC1 antibody immune selection. *Int J Cancer.* 2008;123(6):1357-1363.
18. Surowiak P, Materna V, Maciejczyk A, et al. CD46 expression is indicative of shorter revival-free survival for ovarian cancer patients. *Anticancer Res.* 2006;26(6C):4943-4948.
19. Thorsteinsson L, O'Dowd GM, Harrington PM, Johnson PM. The complement regulatory proteins CD46 and CD59, but not CD55, are highly expressed by glandular epithelium of human breast and colorectal tumour tissues. *APMIS.* 1998;106(9):869-878.
20. Murray KP, Mathure S, Kaul R, et al. Expression of complement regulatory proteins-CD 35, CD 46, CD 55, and CD 59-in benign and malignant endometrial tissue. *Gynecol Oncol.* 2000;76(2):176-182.
21. Kinugasa N, Higashi T, Nouso K, et al. Expression of membrane cofactor protein (MCP, CD46) in human liver diseases. *Br J Cancer.* 1999;80(11):1820-1825.
22. Liszewski MK, Farries TC, Lublin DM, Rooney IA, Atkinson JP. Control of the complement system. *Adv Immunol.* 1996;61:201-283.
23. Tuve S, Wang H, Ware C, et al. A new group B adenovirus receptor is expressed at high levels on human stem and tumor cells. *J Virol.* 2006;80(24):12109-12120.
24. Gaggar A, Shayakhmetov D, Lieber A. CD46 is a cellular receptor for group B adenoviruses. *Nat Med.* 2003;9(11):1408-1412.
25. Sirena D, Lilienfeld B, Eisenhut M, et al. The human membrane cofactor CD46 is a receptor for species B adenovirus serotype 3. *J Virol.* 2004;78(9):4454-4462.
26. Wang H, Liaw YC, Stone D, et al. Identification of CD46 binding sites within the adenovirus serotype 35 fiber knob. *J Virol.* 2007;81(23):12785-12792.
27. Wang H, Liu Y, Li Z, et al. In vitro and in vivo properties of adenovirus vectors with increased affinity to CD46. *J Virol.* 2008;82(21):10567-10579.
28. Liu Y, Wang H, Yumul R, et al. Transduction of liver metastases after intravenous injection of

Ad5/35 or Ad35 vectors with and without factor X-binding protein pretreatment. *Hum Gene Ther.* 2009;20(6):621-629.

29. Anderson BD, Nakamura T, Russell SJ, Peng KW. High CD46 receptor density determines preferential killing of tumor cells by oncolytic measles virus. *Cancer Res.* 2004;64(14):4919-4926.
30. Myers R, Harvey M, Kaufmann TJ, et al. Toxicology study of repeat intracerebral administration of a measles virus derivative producing carcinoembryonic antigen in rhesus macaques in support of a phase I/II clinical trial for patients with recurrent gliomas. *Hum Gene Ther.* 2008;19(7):690-698.
31. Marie JC, Astier AL, Rivailler P, Rabourdin-Combe C, Wild TF, Horvat B. Linking innate and acquired immunity: divergent role of CD46 cytoplasmic domains in T cell induced inflammation. *Nat Immunol.* 2002;3(7):659-666.
32. Abbink P, Lemckert AA, Ewald BA, et al. Comparative seroprevalence and immunogenicity of six rare serotype recombinant adenovirus vaccine vectors from subgroups B and D. *J Virol.* 2007;81(19):4654-4663.
33. Wang SY, Weiner G. Complement and cellular cytotoxicity in antibody therapy of cancer. *Expert Opin Biol Ther.* 2008;8(6):759-768.
34. Coiffier B. Rituximab therapy in malignant lymphoma. *Oncogene.* 2007;26:3603-3613.
35. Idusogie EE, Wong PY, Presta LG, et al. Engineered antibodies with increased activity to recruit complement. *J Immunol.* 2001;166(4):2571-2575.
36. Maloney DG. Follicular NHL, from antibodies and vaccines to graft-versus-lymphoma effects. *Hematology Am Soc Hematol Educ Program.* 2007: 226-232.
37. Zent CS, Secreto CR, Laplant BR, et al. Direct and complement dependent cytotoxicity in CLL cells from patients with high-risk early-intermediate stage chronic lymphocytic leukemia (CLL) treated with alemtuzumab and rituximab. *Leuk Res.* 2008;32(12):1849-1856.
38. Castillo J, Winer E, Quesenberry P. Newer monoclonal antibodies for hematological malignancies. *Exp Hematol.* 2008;36(7):755-768.
39. Dechant M, Weisner W, Berger S, et al. Complement-dependent tumor cell lysis triggered by combinations of epidermal growth factor receptor antibodies. *Cancer Res.* 2008;68(13):4998-5003.
40. Wang M, Fayad L, Cabanillas F, et al. Phase 2 trial of rituximab plus hyper-CVAD alternating with rituximab plus methotrexate-cytarabine for relapsed or refractory aggressive mantle cell lymphoma. *Cancer.* 2008;113(10):2734-2741.
41. Owczarczyk K, Hellmann M, Fliedner G, et al. Clinical outcome and B cell depletion in patients with rheumatoid arthritis receiving rituximab monotherapy in comparison with patients receiving concomitant methotrexate. *Ann Rheum Dis.* 2008;67(11):1648-1649.
42. Petereit H, Rubbert-Roth A. Rituximab levels in cerebrospinal fluid of patients with neurological autoimmune disorders. *Mult Scler.* 2009;15(2): 189-192.
43. Yang YW, Lin WC, Wu MS, Lee PH, Tsai MK. Early diagnosis and successful treatment of acute antibody-mediated rejection of a renal transplant. *Exp Clin Transplant.* 2008;6(3):211-214.
44. Di Paolo N, Ni S, Gaggar A, et al. Evaluation of adenovirus vectors containing serotype 35 fibers for tumor targeting. *Cancer Gene Ther.* 2006; 13(12):1072-1081.
45. Ni S, Bernt K, Gaggar A, Li ZY, Kiem HP, Lieber A. Evaluation of biodistribution and safety of adenovirus vectors containing group B fibers after intravenous injection into baboons. *Hum Gene Ther.* 2005;16(6):664-677.
46. Sakurai F, Nakamura S, Akitomo K, et al. Transduction properties of adenovirus serotype 35 vectors after intravenous administration into nonhuman primates. *Mol Ther.* 2008;16(2):726-733.